

Brief Reports

*Brief Reports are accounts of completed research which, while meeting the usual **Physical Review** standards of scientific quality, do not warrant regular articles. A Brief Report may be no longer than four printed pages and must be accompanied by an abstract. The same publication schedule as for regular articles is followed, and page proofs are sent to authors.*

Theory of the Fermi-level energy in semiconductor superlattices

James H. Luscombe

Central Research Laboratories, Texas Instruments Incorporated, Dallas, Texas 75265

Raj Aggarwal

*Central Research Laboratories, Texas Instruments Incorporated, Dallas, Texas 75265
and Department of Electrical Engineering and Computer Science,
Massachusetts Institute of Technology, Cambridge, Massachusetts 02139*

Mark A. Reed

*Central Research Laboratories, Texas Instruments Incorporated, Dallas, Texas 75265
and Department of Electrical Engineering, Yale University, New Haven, Connecticut 06520*

William R. Frensley

*Central Research Laboratories, Texas Instruments Incorporated, Dallas, Texas 75265
and Department of Electrical Engineering, University of Texas at Dallas, Richardson, Texas 75083*

Marshall Luban

*Department of Physics and Astronomy and Ames Laboratory, Iowa State University, Ames, Iowa 50011
(Received 22 April 1991)*

A theoretical study of the properties of the Fermi level in semiconductor superlattices (SL's) is made which is based upon the carrier occupation of the minibands in thermal equilibrium. We find, for a fixed carrier density and temperature, that the SL Fermi level can differ significantly from that obtained using commonly employed three-dimensional approximations, depending upon the relative spacings and widths of the minibands, with the SL Fermi level being higher than the corresponding bulk value. We find that the SL Fermi level is a sensitive function of the relative widths of the quantum wells and barriers.

In recent years, there has been renewed interest in semiconductor superlattices, most notably in their transport properties.¹⁻⁸ The artificial periodicity of the superlattice (SL) perturbs the band structures of the underlying materials to produce new (miniband) conduction states, the energies of which can be selectively tuned through the design of the SL. While there has been much effort, both experimental and theoretical, aimed at elucidating the allowed states of SL's, there has been surprisingly little attention devoted to the thermal occupation of these states.

In this article, we investigate the properties of the Fermi-level energy for semiconductor SL systems. Despite the central importance of the Fermi-level energy, experimental results on SL systems are often interpreted by assuming a bulk, three-dimensional Fermi-level value, or at best, by making educated guesses for which minibands are occupied. To our knowledge, however, there has not been a systematic study of the SL Fermi level. As

we show, the actual Fermi level for a SL can differ significantly from that obtained using bulk approximations, depending upon the relative spacings and widths of the minibands. This is related to the fact that the density of states for a SL is a hybrid between a two- and a three-dimensional density of states, and a calculation of the Fermi level must reflect this difference. We first calculate the Fermi level for a given density of carriers which occupy the minibands of a SL in thermal equilibrium. We find that, for the same density and temperature, the SL Fermi level is higher than the corresponding bulk Fermi level. We then investigate the dependence of the Fermi level upon the parameters of the SL (e.g., the relative widths of the quantum wells and barriers), for a fixed carrier density.

In the following, we adopt several simplifying assumptions which allow the basic effects of the SL minibands on the Fermi-level energy to be most readily ascertained. We assume the carriers to be a noninteracting Fermi gas

which populate the energy levels of the system, an assumption which is commonly employed in determining the Fermi level in bulk, homogeneous semiconductor systems. We assume that the SL quantum potential [$V(z)=V(z+a)$, where a is the period of the SL] is known from the conduction-band minima of the host materials, in terms of which a set of miniband energies can be obtained. We further assume that the SL dispersion relation can be written

$$E_j(k_1, k_z) = \frac{\hbar^2}{2m^*} k_1^2 + \varepsilon_j(k_z a), \quad j=1, 2, \dots \quad (1)$$

where $\hbar k_1$ is the momentum transverse to the SL direction, k_z is the longitudinal wave vector, and the ε_j are the miniband dispersion relations, with j the band index. We

$$\rho(z; E_F) = \frac{1}{2\pi^2} \sum_j \int_0^\infty k_1 dk_1 \int_{-\pi/a}^{\pi/a} dk_z |\psi_{j, k_z}(z)|^2 (1 + \exp\{\beta[E_j(k_1, k_z) - E_F]\})^{-1} \quad (2)$$

where $\psi_{j, k_z}(z)$ is the single-particle Bloch wave function associated with the j th miniband, normalized according to

$$\frac{1}{a} \int_0^a |\psi_{j, k_z}(z)|^2 dz = 1, \quad (3)$$

and $\beta \equiv (k_B T)^{-1}$. Note that the electron density $\rho(z)$ is in principle inhomogeneous through the behavior of the wave functions. Physically, this corresponds to an increase in the carrier density in the quantum wells of the SL, and to a decrease in the barriers. The magnitude of such spatial inhomogeneities in the carrier density cannot be accurately modeled without a self-consistent calculation of the electron states, where the inhomogeneous charge distribution generates (via Poisson's equation) the potential from which the minibands are determined.¹⁰ We will not attempt such a coupled Poisson-Schrödinger calculation here; rather we adopt the simplest (and commonly employed) approximation where the minibands are obtained from the "flat-band" potential V , described above. Note that, whatever the form of the SL potential from which the minibands are derived, to determine the Fermi level we require only the total density of carriers,

$$n(E_F) \equiv \frac{1}{a} \int_0^a \rho(z; E_F) dz, \quad (4)$$

and hence any inhomogeneities in the charge distribution are averaged out.

Thus, substituting (1) into (2), integrating over (2) as in (4), utilizing (3) and integrating over the transverse degrees of freedom, we obtain

$$n = \frac{n_{2D}}{a} \sum_j L_j, \quad (5)$$

where $n_{2D} \equiv m^* / (\pi \beta \hbar^2)$ and

$$L_j \equiv \frac{1}{2\pi} \int_{-\pi}^{\pi} dx F_0[\beta(E_F - \varepsilon_j(x))]. \quad (6)$$

Here F_0 is the Fermi-Dirac integral for a two-

dimensional density of states, $F_0(y) = \ln[1 + \exp(y)]$. Equations (5) and (6) generalize the form of the expression for the density of a two-dimensional electron gas: an integration is performed (instead of summation) over the miniband energies which result from the splittings induced by the interactions among the quantum wells of the SL. Once the minibands are specified, we can infer via (5) and (6) the Fermi level which corresponds to a given density of carriers.

While it is possible to solve for the band structure of the minibands for a given SL potential, we have, for simplicity, adopted a model dispersion relation¹¹ to represent each miniband, of the form

$$\varepsilon_j(x) = \varepsilon_{j,0} - W_j \cos(x), \quad (7)$$

where $\varepsilon_{j,0}$ is the center energy of miniband j and $2W_j$ is the respective bandwidth. These parameters are assumed known,¹² and are taken as input for the present study. The tight-binding form in (7) is a convenient example of a one-dimensional band structure. If necessary, it would be a simple matter to numerically integrate (6) using more accurate minibands. We have calculated Kronig-Penney minibands and find results which are well parametrized by the form of (7).

With (7) substituted in (6), the resulting integral appears to be intractable except for one case for which we can obtain useful analytic results. When the Fermi level does not intersect a miniband, i.e., $|E_F - \varepsilon_{j,0}| > W_j$, it can readily be shown that L_j possesses the following rapidly convergent expansion:

$$L_j = F_0(\beta(E_F - \varepsilon_{j,0})) + \sum_{k=1}^{\infty} \frac{(-1)^{k+1}}{k} e^{-\beta k |E_F - \varepsilon_{j,0}|} [I_0(k\beta W_j) - 1] \quad (8)$$

where I_0 is a modified Bessel function. When E_F intersects a miniband, however, we have not found a useful analytic expression for L_j . For the general case (no restriction on E_F), we have numerically integrated the com-

bined equations (6) and (7). Equation (8) provides a useful check on numerical results when applicable.

Equation (5) defines an implicit relationship between the Fermi level and the total density of carriers in the SL minibands. In order to accurately describe the equilibrium density of carriers in the SL states, however, the analysis must include a description of all the states available to carriers with energies lying in the vicinity of the Fermi level. For any given semiconductor system, there are numerous possible physical processes which can affect the free carrier density.¹³ For example, carrier freezeout may occur if the impurity states are sufficiently localized. In semiconductors with a small effective mass such as GaAs, however, one would expect that the mutual screening of the impurity potentials prevents the localization of hydrogenic states for doping densities above a characteristic value. (Deep levels can still be a major effect, as in the well-known “DX-center” problem.) Below, we adopt the simplest assumption of a monovalent donor species which remains ionized independent of the Fermi level, and thus the carrier density equals the donor concentration. In GaAs systems, this is found to be a good approximation for donor concentrations above the low 10^{16} - cm^{-3} range;¹⁴ donor densities in experimental GaAs SL’s are commonly well above this value, with $2 \times 10^{18} \text{ cm}^{-3}$ being typical.

Shown in Fig. 1 are our results for the density versus Fermi level for a GaAs/Al_{0.3}Ga_{0.7}As SL with 50 Å quantum wells and 70-Å barriers obtained with use of (5) and (7). The energies of the three lowest minibands (relative to the bulk GaAs conduction-band minimum) are shown at the top of the figure in crosshatch. The miniband energy extrema [which are used to infer the parameters in (7)], were obtained using a Kronig-Penney model incorporating the effective mass discontinuities,¹⁵ together with a 65% conduction-band offset. The SL density of carriers is shown as a function of Fermi level, together with that for bulk¹⁶ GaAs at two different temperatures,

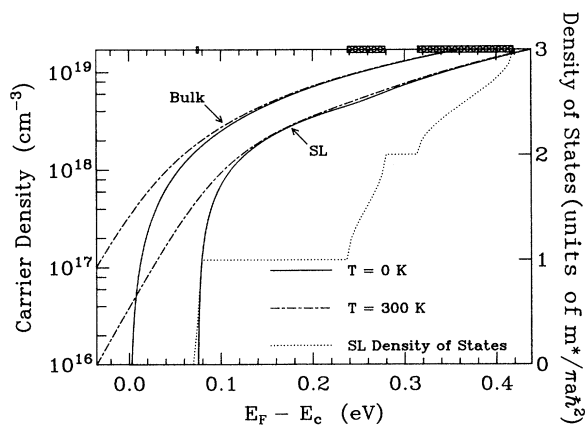


FIG. 1. Density vs Fermi level (left ordinate) for GaAs/Al_{0.3}Ga_{0.7}As superlattice and for bulk GaAs for two temperatures. Three lowest miniband energies (relative to GaAs conduction-band minimum) are shown at top in cross-hatch. Superlattice has 50-Å GaAs quantum wells and 70-Å barriers of GaAs Al_{0.3}Ga_{0.7}As. Superlattice density of states shown in dotted line (right ordinate).

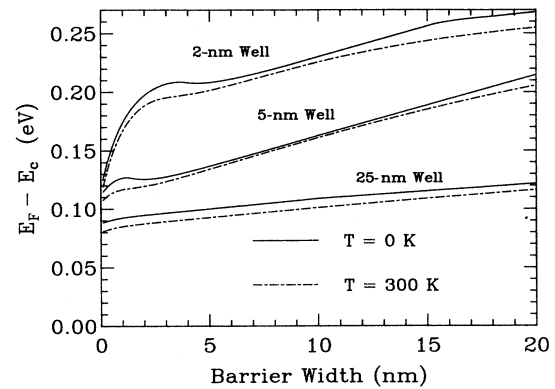


FIG. 2. Superlattice Fermi level for fixed carrier density ($2 \times 10^{18} \text{ cm}^{-3}$) as a function of superlattice parameters for two temperatures. For each curve the quantum-well width is held fixed, and the barrier width is varied.

$T=0 \text{ K}$ (solid lines) and $T=300 \text{ K}$ (dash-dotted line). It is seen that for a given density and temperature, the SL Fermi level exceeds the corresponding bulk Fermi level by approximately the energy of the lowest miniband. We have also shown the SL density of states (dotted line). The quantized, “staircase” appearance resembles a two-dimensional density of states, in that between minibands there are no additional states for SL transport. As the Fermi level exceeds each miniband minimum, however, the density of states suddenly acquires a three-dimensional character.

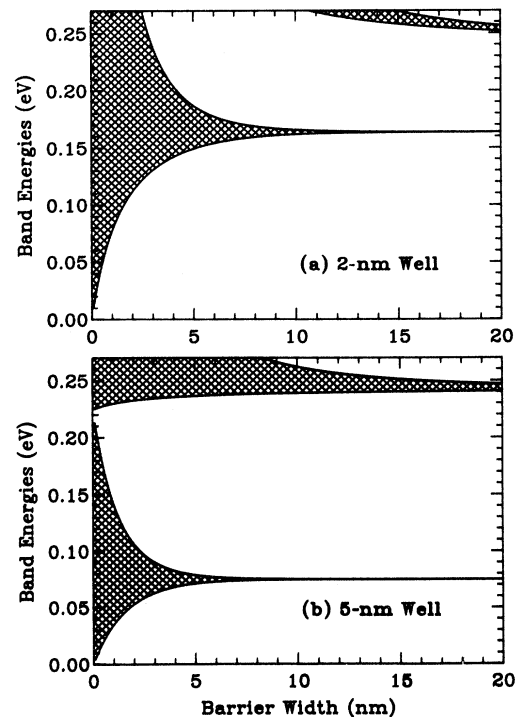


FIG. 3. Miniband energies as a function of SL parameters. Each panel corresponds to superlattices of varying barrier width, but fixed quantum-well width.

Figure 2 shows the behavior of the Fermi level which results for a fixed density of carriers ($2 \times 10^{18} \text{ cm}^{-3}$) as a function of the SL parameters. Three sets of curves are shown. Each set corresponds to a sequence of SL systems for two temperatures in which the quantum-well width is held fixed, but in which the barrier width is allowed to vary. Note that for each set of SL parameters in Fig. 2, a separate determination of the miniband parameters is required. In the limit as the barrier width vanishes, the SL becomes bulk material, and the Fermi level evolves to the appropriate bulk value, that for GaAs in this instance. The barrier material in all cases is $\text{Al}_{0.3}\text{Ga}_{0.7}\text{As}$.

It will be noted from Fig. 2 that the Fermi level is not always a monotonic function of the SL parameters. This can be traced to the qualitative behavior of the minibands as a function of barrier width, such as is shown in Fig. 3. Starting from zero, as the barrier width is made finite, the bulk conduction band is quantized into a series of minibands by the SL periodicity. For small barrier widths, the first miniband is rather wide in energy. However, a small energy gap is opened up between the bulk conduction-band minimum and bottom of the first miniband. To populate the SL with the same density of carriers, therefore, the Fermi level must increase accordingly to overcome this energy gap. As the barriers are made wider, the minibands tend to shrink in bandwidth (from above as well as from below), and thus the Fermi level must *generally* be an increasing function with increasing barrier widths to populate the ever-narrowing minibands with the same carrier density. Some interesting exceptions can occur, however. If, as a function of increasing barrier width, the top of the (shrinking) miniband which contains the Fermi level, meets, and then crosses beneath

the (rising) Fermi level, E_F can then either "plateau" or even decrease in value, being "pulled down" by the top of the shrinking miniband. This is seen to occur in Fig. 3 at barrier widths of approximately 4 and 2 nm, respectively, for well widths of 2 and 5 nm. From Fig. 3(a), we also observe a change in the behavior of the Fermi level as it crosses into the second miniband at a barrier width of approximately 15 nm. Note that these effects are accentuated in the case of the smallest quantum-well width shown, where the relative influence of an increasing barrier width is strongest.

In conclusion, we have investigated theoretically the properties of the Fermi level in semiconductor superlattices, based upon the thermal occupation of the minibands. For calculational simplicity, we have employed a tight-binding band structure, (7), for the minibands, a condition which can be trivially relaxed in the light of more realistic minibands. We find that the SL Fermi level differs from that obtained using bulk approximations owing to the energy gaps between minibands, and that the difference can be significant depending upon the relative spacings and widths of the minibands.

This work was sponsored in part by the Office of Naval Research, Contract No. N00014-87-C-0363, Quantum Device Development, and in part by Wright Laboratories, Contract No. F33615-89-C-1074, Resonant Tunneling Transistor Logic. Ames Laboratory is operated for the U. S. Department of Energy by Iowa State University under Contract No. W-7405-Eng-82, Office of Basic Energy Sciences. We are grateful to Alan Seabaugh for his insightful comments.

¹See, for example, *Physics and Applications of Quantum Wells and Superlattices*, edited by E. E. Mendez and K. von Klitzing (Plenum, New York, 1988).

²B. Deveaud, J. Shah, T. C. Damen, B. Lambert, and A. Regreny, *Phys. Rev. Lett.* **58**, 2582 (1987).

³T. Duffield, R. Bhat, M. Koza, F. DeRosa, K. M. Rush, and S. J. Allen, *Phys. Rev. Lett.* **59**, 2693 (1987).

⁴R. A. Davies, M. J. Kelly, and T. M. Kerr, *Phys. Rev. Lett.* **55**, 1114 (1985).

⁵R. J. Aggarwal, M. A. Reed, W. R. Frensley, Y. C. Kao, and J. H. Luscombe, *Appl. Phys. Lett.* **57**, 707 (1990).

⁶P. England, J. R. Hayes, E. Colas, and M. Helm, *Phys. Rev. Lett.* **63**, 1708 (1989).

⁷M. A. Kinch and A. Yariv, *Appl. Phys. Lett.* **55**, 2093 (1989).

⁸R. A. Davies, D. J. Newson, T. G. Powell, M. J. Kelly, and H. W. Myron, *Semicond. Sci. Technol.* **2**, 61 (1987).

⁹See, for example, H. J. Kreuzer, *Nonequilibrium Thermodynamics and Its Statistical Foundations* (Oxford, New York, 1981), p. 212.

¹⁰Such a calculation is currently underway. A. M. Bouchard, J. H. Luscombe, and M. Luban (unpublished).

¹¹During completion of this work, we became aware that (7) was used in Ref. 8 to compute the Fermi level for these authors' SL structures. However, they do not present analytic results, nor is a systematic study made of the properties of a SL Fermi level. For the structures listed, we obtain results basically in agreement with those presented in Ref. 8.

¹²These parameters could be obtained either theoretically using an assumed model of the SL potential, or they could be inferred from experiment.

¹³See, for example, J. S. Blakemore, *Semiconductor Statistics* (Dover, New York, 1987), Chap. 3.

¹⁴J. Basinski and R. Olivier, *Can. J. Phys.* **45**, 119 (1967).

¹⁵See, for example, G. Bastard, *Phys. Rev. B* **24**, 5693 (1981).

¹⁶The latter results were obtained with standard expressions for a finite-temperature three-dimensional electron gas. See, for example, J. S. Blakemore, *Solid-State Electron.* **25**, 1067 (1982).